7th International Conference on Debris-Flow Hazards Mitigation

Numerical simulation of debris flows focusing on the behavior of fine sediment

Yuichi Sakai[a,*], Norifumi Hotta[a]

[a]*Graduate School of Agricultural and Life Sciences, The University of Tokyo, Tokyo, Japan*

Abstract

Debris flows generally includes a wide range of grain sizes, in which fine sediment behaves as a fluid phase rather than as a solid phase and enlarges the pore fluid density. Although in existing models fine sediment constantly behave as fluid phase from initiation to deposition, previous researches have reported that behavior of fine sediment can vary through debris-flow propagations depending on the kinematic conditions (i.e., relation of turbulence and the settling velocity of the particles). To test the effects of this transitional behavior of fine sediment and compare with existing models, we conduct numerical simulations of debris flows with bidisperse granular materials, employing two models for the behavior of small particles: (i) all small particles constantly behave as a fluid phase (Model I); and (ii) the ratio of small particles behaving as a fluid phase varies depending on the kinematic conditions (Model II). In the simulations, we used an inclined channel with erodible bed at the upper stream end of the reach, where debris flows initiate by supplying water. Varying the inclination from 15° to 20°, we measured the time series of discharges, flow depths, sediment concentrations and pore fluid densities at the downstream end. Hydrographs of the two models are significantly different at higher slopes, with a sharp peak at the front of debris flows in Model I and relatively moderate peak in Model II. These differences are caused by higher pore fluid densities from the front to the tail of debris flows in Model I, in contrast to lower pore fluid densities in Model II, where not all of small particles behave as a fluid phase. This infers that discharge rate of debris flows can be overestimated especially at higher slopes if the transitional behavior of fine sediment is not considered.

Keywords: debris flow; numerical simulation; fine sediment; pore fluid density; hydrograph

1. Introduction

Debris flows are mixtures of water and sediment descending steep slopes in mountainous regions: these phenomena can cause severe damage to human life and property. Numerical simulations of debris flows have been used to prevent and mitigate sediment disasters related to debris flows. Previous studies have explored the numerical simulation of debris flow using flow resistance formula (Iverson, 1997) and entrainment rate equations (Iverson and Ouyang, 2015), which reflect the physical characteristics of the flow. Flow resistance formula are derived based on the constitutive equations for debris flows, which are modeled under the assumption that sediment particles are of uniform grain size (Takahashi, 1991; Egashira et al., 1997; Berzi and Jenkins, 2008). The performance of these numerical simulation models has been validated by laboratory measurements of the characteristics of monogranular debris flows, and good agreement with the calculation results has been reported (Egashira et al., 2001; Berzi and Larcan, 2013).

In contrast, natural debris flows comprise a wide range of grain sizes, from clay and silt to boulders (Coe et al., 2008): this variation partly determines flow characteristics such as the segregation of coarse grains to the flow surface (Takahashi et al., 1992) and the suspension of fine sediment in pore fluid (Iverson, 1997; Kaitna et al., 2016). The pore fluid of debris flows can be made turbulent by strong shear of coarse sediment particles (Hotta, 2011), such that fine sediment may contribute to the pore fluid as a fluid phase (Hotta et al., 2013). Thus, numerical simulations of natural debris flows must take into account the increase in pore fluid density that can result from the suspension of fine sediment (Osti et al., 2004; Osti and Egashira, 2008). In early simulations, pore fluid density was generally assumed

* Corresponding author e-mail address*: sakai@fr.a.u-tokyo.ac.jp*

to be constant throughout debris-flow propagation, in the absence of clear selection criteria to determine pore fluid density. Recently, numerical simulations of *in situ* debris flows containing fine sediment have considered the critical diameter of the sediment particles, below which sediment particles contributes to a fluid phase, accordingly varying the pore fluid densities through debris flow propagations (Nishiguchi et al., 2011; Uchida et al., 2013). This have led to a higher reproducibility of the propagation behavior of such debris flows.

Although introducing the critical diameter made it clearer how to set the pore fluid density, fine sediment behaving as a fluid phase was determined simply by a given grain size. However, recent research from laboratory experiments using bidisperse granular materials has shown that fine sediment does not necessarily behave as a fluid phase (Hotta et al., 2013), or rather, the behavior of fine sediment depends on the kinematic conditions, i.e. the ratio of shear or turbulent velocity to the settling velocity of fine sediment (Nakatani et al., 2018; Sakai et al., 2019). In other word, this implies that the behavior of the fine sediment is not simply determined by the grain size, and fine sediment may behave as a solid or fluid phase depending on the kinematic conditions even with the same grain size.

In this study, we constructed a numerical simulation model incorporating these fine sediment behaviors and tested its performance for debris flows with bidisperse granular materials, comparing with the numerical simulation based on the existing method in which fine sediment behaving as a fluid phase was determined simply by a given grain size.

2. Numerical simulation of debris flows focusing on fine sediment behavior

2.1. Governing equations for debris flows consisting of bidisperse granular materials

The one-dimensional behavior of debris flows consisting of bidisperse granular materials is described based on the following governing equations, i.e., continuity equations for debris flow with large and small particles and the momentum equation for debris flow:

$$\frac{\partial h}{\partial t}+\frac{\partial M}{\partial x}=E \tag{1}$$

$$\frac{\partial (C_L h)}{\partial t}+\frac{\partial (C_L M)}{\partial x}=E(1-r)C_* \tag{2}$$

$$\frac{\partial (C_S h)}{\partial t}+\frac{\partial (C_S M)}{\partial x}=ErC_* \tag{3}$$

$$\frac{\partial M}{\partial t}+\beta\frac{\partial (uM)}{\partial x}=-gh\frac{\partial H}{\partial x}-\frac{\tau_0}{\rho_m}. \tag{4}$$

where t is time, x is the coordinate axis along the flow direction, h is the flow depth, M is the discharge rate at a unit width, E is the entrainment rate at the bed, C_L and C_S are the depth-averaged sediment concentration of large and small particles in the cross section, C_* is the concentration of the sediment mixture in the channel deposits, r is the ratio of entrained small particles to the entrained bidisperse granular mixture, β is the momentum correction factor, u is the depth-averaged velocity, g is the acceleration due to gravity, H is the elevation of the flow surface, τ_0 is the shear stress at the bed, and ρ_m is the density of the debris flow.

There are several existing resistance formula and entrainment rate equations of debris flows. The flow resistance formula proposed by Egashira et al. (1997) is employed for τ_0:

$$\tau_0=\tau_{0y}+\rho f_b u^2 \tag{5}$$

$$\tau_{0y}=\left(\frac{C_d}{C_*}\right)^{\frac{1}{5}}(\sigma-\rho)C_d gh\cos\theta\tan\phi_s \tag{6}$$

$$f_b=\frac{25}{4}\left\{k_g\frac{\sigma}{\rho}(1-e^2){C_d}^{\frac{1}{3}}+k_f\frac{(1-C_d)^{\frac{5}{3}}}{{C_d}^{\frac{2}{3}}}\right\}\left(\frac{h}{d}\right)^{-2}. \tag{7}$$

where ρ is the density of the pore fluid, σ is the density of the sediment particles, C_d is the concentration of sediment particles behaving as a solid phase, θ is the bed inclination, ϕ_s is the internal friction angle of the sediment particles, k_g is a constant (= 0.0828), e is the coefficient of the restitution of the sediment particles, k_f is the constant relating to interstitial space, and d is the representative diameter of particles in sediment mixture.

The entrainment rate equation proposed by Egashira et al. (2001) is employed for E:

$$E = u\tan(\theta - \theta_e) \tag{8}$$

$$\tan\theta_e = \frac{C_d(\sigma/\rho - 1)}{C_d(\sigma/\rho - 1) + 1}\tan\phi_s. \tag{9}$$

Equation (8) employs the concept of equilibrium bed slope θ_e for a given sediment concentration expressed in Eq. (9), where erosion and deposition are balanced. The surface position of the river bed varies through erosion and deposition such that slope θ approach θ_e.

In this framework, the suspension of small particles affects the flow resistance and entrainment rate through the changes in the sediment concentration behaving as solid phase, the pore fluid density and the representative diameter. Details of this point are discussed in the next section.

2.2. Models for the behavior of fine sediment

As coarse sediment contributes to inter-particle stress, fine sediment contributes to the stress on the pore fluid, increasing its density. Among bidisperse granular materials containing large particles that constantly behave as a solid phase, small particles can behave as both a solid and a fluid phase. Thus, modeling the behavior of small particles may affect the overall results of numerical simulations. In this study, we defined two models for the behavior of small particles: (i) all small particles constantly behave as a fluid phase (Model I); and (ii) the ratio of small particles behaving as a fluid phase varies depending on the kinematic conditions (Model II) (Fig. 1). In Model II, the sediment concentration of small particles (C_S) is divided into that behaving as a fluid phase (C_f) and a solid phase ($C_S - C_f$).

Model I reflects the conventional treatment of fine sediment, with the threshold decided simply by the grain size. In Model I, the pore fluid density ρ and representative diameter d are expressed as $\rho_{Model\,I} = \rho_w\,(1 - C)/(1 - C_L) + \sigma\,C_S/(1 - C_L)$ and $d_{Model\,I} = d_L$, where C is the sediment concentration of the bidisperse granular mixture ($C_L + C_S$) and ρ_w is the density of water.

Model II adopts the concept that the behavior of small particles depends on the kinematic conditions, i.e., the ratio of shear velocity $u_* = \sqrt{gh\sin\theta}$ or turbulent velocity of the pore fluid $v_t = 5/2\sqrt{k_f}((1 - C_L)/C_L)^{1/3}\,ud_L/h$ to the settling velocity of small particles $w_s = ((1 - C)/(1 - C_L))^n w_0$, where n is an empirically determined exponent (for simplicity, $n = 4$ in this study) and w_o is the terminal settling velocity of a single particle. v_t is derived from the constitutive equations of Egashira et al. (1997), which assume that the mixing length contributing to the Reynolds stress is defined by the scale of the pore space between particles.

Through flume tests with bidisperse granular materials, Sakai et al. (2019) derived linear-regression based relationships between the behavior of small particles and the kinematic conditions, u_*/w_s or v_t/w_s, using the blending factor α, which is defined as $f_{ex} = (1 - \alpha)f_{cal:Model\,1} + \alpha f_{cal:Model\,2}$ through the comparison between the experimental and theoretical friction coefficients of steady-state debris flows. The experimental friction coefficient of debris flows is $f_{ex} = 2gh\sin\theta/u^2$ and the theoretical friction coefficients for Models 1 and 2 in Sakai et al. (2019) are $f_{cal:Model\,1} = 25/(2\rho_m)K(\rho_w, C)(h/d_m)^{-2}$ and $f_{cal:Model\,2} = 25/(2\rho_m)K(\rho_f,\, C_L)(h/d_L)^{-2}$, where $K(\rho, C_d)$ is the function of the pore fluid density and concentration of sediment particles behaving as a solid phase, the volume-averaged diameter of bidisperse granular mixtures $d_m = (d_L C_L + d_S C_S)/(C_S + C_L)$ and the pore fluid density with all small particles suspended $\rho_f = \rho_w\,(1 - C)/(1 - C_L) + \sigma\,C_S/(1 - C_L)$. In Models 1 and 2, all small particles behave as solid and fluid phases, respectively (see Sakai et al. (2019) for further details). The relationships between α and u_*/w_s or v_t/w_s are expressed as follows:

$$\alpha = 0.0175\,u_*/w_s - 0.0374 \tag{10}$$

$$\alpha = 0.0167\,v_t/w_s - 0.0457. \tag{11}$$

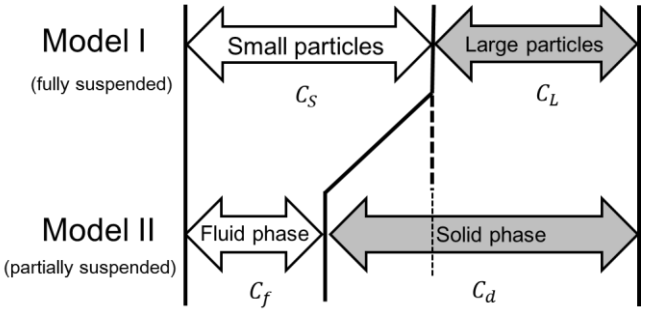

Fig. 1. Conceptual diagram of Models I and II for the behavior of small particles.

As seen from the definition, α cannot be used directly to calculate the fraction of small particles behaving as a fluid phase, such as $C_f = \alpha C_S$. To do so, we need to derive the relationship between α and α' define α' as the ratio of sediment particles behaving as a fluid phase to all small particle. The definition of α can be approximated as follows under the assumption that the friction coefficient is less sensitive to the changes of the pore fluid density and sediment concentration behaving as solid phase in the function $K(\rho, C_d)$ compared to the change of the representative diameter, i.e., $K(\rho, C_L) \approx K(\rho, C_d)$:

$$f_{ex} = (1-\alpha) f_{cal:Model\ 1} + \alpha f_{cal:Model\ 2} = \frac{25}{2\rho_m}\left\{(1-\alpha)K(\rho_w, C)\left(\frac{h}{d_m}\right)^{-2} + \alpha K(\rho_f, C_L)\left(\frac{h}{d_L}\right)^{-2}\right\}$$
$$\simeq \frac{25}{2\rho_m}\frac{K(\rho_f,\ C_L)}{h^2}\left\{(1-\alpha)\left(\frac{C_L d_L + C_S d_S}{C_L + C_S}\right)^2 + \alpha {d_L}^2\right\}. \quad (12)$$

Using α', Eq. (12) is rewritten as

$$f_{ex} = \frac{25}{2\rho_m}\frac{K(\rho,\ C_d)}{h^2}\left(\frac{C_L d_L + (1-\alpha')C_S d_S}{C_L + (1-\alpha')C_S}\right)^2. \quad (13)$$

Using Eqs. (12) and (13) under the assumption $K(\rho_f, C_L) \approx K(\rho, C_d)$, we obtain the following relationship between α and α':

$$\alpha' = 1 - \frac{d_L - D}{D - d_S}\frac{C_L}{C_S} \quad (14)$$

$$D = \frac{\sqrt{(1-\alpha)\,(C_L d_L + C_S d_S)^2 + \alpha (C_L + C_S)^2 {d_L}^2}}{C_L + C_S}. \quad (15)$$

Thus, the concentration of sediment particles behaving as a fluid phase C_f and solid phase C_d are expressed as

$$C_f = \alpha' C_S \quad (16)$$

$$C_d = C_L + C_S - C_f \quad (17)$$

and the density of the pore fluid ρ and the representative diameter d are

$$\rho_{Model\ II} = \rho_w \frac{1 - C_d - C_f}{1 - C_d} + \sigma \frac{C_f}{1 - C_d} \quad (18)$$

$$d_{Model\ II} = \frac{d_L C_L + d_S (C_S - C_f)}{C_d}. \quad (19)$$

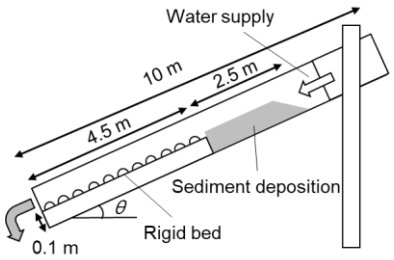

Fig. 2. Schematic diagram of the channel used in Sakai et al. (2019).

Table 1. Physical parameters used in the numerical simulation.

Density of water: ρ_w (g/cm^3)	1.00
Density of sediment particles: σ (g/cm^3)	2.60
Internal friction angle of the sediment particles: ϕ_s (°)	38.5
Coefficient of the restitution of the sediment particles: e	0.85
Concentration of the sediment mixture in the channel deposition C_*	0.70
Constant relating to interstitial space: k_f	0.08

2.3. Numerical conditions

Numerical simulations were using the flume test configuration used by Sakai et al. (2019), as shown in Fig. 2. The channel was 10 m in length and 0.1 m wide. At 4.5 m from the downstream end, the channel floor was raised to a height of 10 cm, and 2.9-mm grains were glued to the rigid bed to provide bed roughness. Sediment comprising bidisperse granular mixtures was deposited upstream of the rigid bed to the height of the bed roughness surface to form an erodible bed. We selected bidisperse granular mixtures of 2.9-mm and 0.11-mm grains at a mixing ratio of 4:1 for the deposited materials at the upper stream. The maximum sediment concentration of the flowing particles was set to the value of the concentration of the sediment deposition at the channel deposition. Small particles are assumed to behave as solid phase when they are deposited and can behaves as fluid phase only after entrainment into the flow. For the erosion process, r is assumed to be the same value as the ratio of small particles to the deposited bidisperse granular mixtures. The inclination of the channel was 15° in the original literature; however, we varied this inclination from 15° to 20° for sensitivity analysis. Water was supplied from the upstream end at the constant rate of 3,000 cm^3/s for 20 s. At the downstream end, we measured a time series of discharges, flow depths, pore fluid densities, and sediment concentration of bidisperse granular mixtures, small particles, and small particles behaving as a fluid phase. We applied a leapfrog scheme for calculations on a staggered grid, with a temporal resolution of 0.0005 s and spatial resolution of 0.5 cm. The physical parameters used in the numerical simulation are listed in Table 1.

3. Results and Discussion

The calculations by Models I and II were compared to test their performance and investigate the sensitivity, showing the calculated results for channel inclinations of 15° and 20° as representative cases in this section. The time series of discharges calculated by Models I and II are compared in Fig. 3, where both models showed sharper peaks at higher inclinations. Model I showed the highest peak among the three calculated results at all inclinations, followed by Model II with u_*/w_s. Model II with v_t/w_s exhibited lower peak discharges and relatively smoother changes between peaks, which occurred later than those of the other two model results. Differences in the calculated hydrographs between Model I and Model II with v_t/w_s were larger at higher slopes. Since the amount of water supplied was constant, differences between hydrographs are mainly attributed to differences in the degree of entrainment from upstream sediment deposition, which is affected by pore fluid density through changes in the equilibrium slope in Eq. (9).

The time series of flow depths calculated by Models I and II are compared in Fig. 4. Although the timing of the peaks in Model I and Model II with u_*/w_s were different from those of Model II with v_t/w_s, their overall performance was relatively close in contrast to that of the discharge results.

Figure 5 shows the time series of pore fluid density calculated by Models I and II. Pore fluid density had the highest values at the flow front, and then decreased with density of water. This result corresponds to the trend in discharge, which also had a peak at the flow front. In Model II with v_t/w_s, pore fluid density was small compared to that in Models I and II with u_*/w_s at an inclination of 15°, whereas this difference became small at higher slopes. The maximum value of the pore fluid densities reached about 1.5 g/cm^3, which are achieved when the sediment concentration of bidisperse granular materials becomes its maximum value and all small particles included in them behaves as a fluid phase, as shown in the calculation by Model I with an inclination of 20°.

Since pore fluid densities directly corresponds to the behavior of small particles, the ratio of small particles behaving as a fluid phase should be investigated. Fig. 6 shows the time series of concentrations of sediment mixtures, small particles, and small particles behaving as a fluid phase. This indicates that the behavior of small particles estimated by Model II varies with debris flow propagations.

The difference between Models I and II is detected in the above calculations, especially at higher slopes. Model I may have overestimated the hydrograph compared to Model II because not all small particles actually behave as a fluid phase (Sakai et al., 2019). Model II performed better than Model I, but exhibited different performance depending on the kinematic conditions, i.e., u_*/w_s or v_t/w_s. Model II with u_*/w_s and v_t/w_s have several advantages and disadvantages. Although u_*/w_s is easily incorporated into the model by the simple expression u_*, it is important to remember that u_* reflect the external stress exerted on debris flow and does not directly reflect the Reynolds stress, which lead to the suspension of small particles in the pore fluid. In contrast, v_t strictly reflects the Reynolds stress of the pore fluid. For this reason, Model II with v_t/w_s seems to be a stricter model; however, it should be noted that v_t can exhibit unstable behavior when the sediment concentration approaches zero, as seen from its expression.

To investigate the sensitivity of u_* and v_t, the time series of u_* and v_t calculated by Model II with u_*/w_s and v_t/w_s are compared in Fig. 7, which shows opposite trends in u_* and v_t. This results is attributed to the flow depths at which u_* and v_t exhibit opposite behavior: u_* corresponds directly to the flow depth, whereas v_t corresponds inversely to the flow depth. The flow depth was most sensitive to u_* and v_t, and the sediment concentration has relatively little effect on v_t. The sharp peak of v_t at the debris flow front is also attributed to small flow depth values. These behavior of u_* and v_t in turn affect pore fluid density through the suspension of small particles.

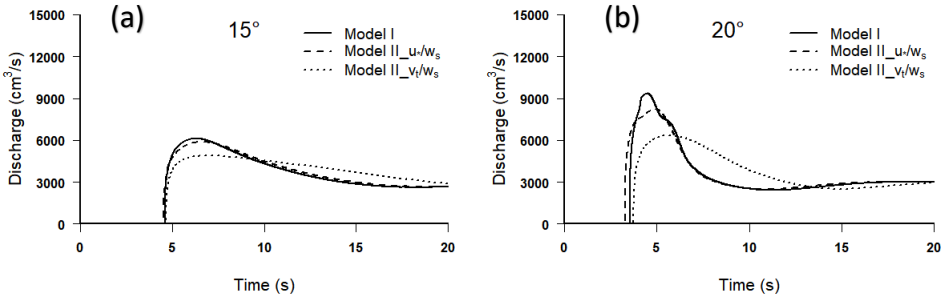

Fig. 3. Time series of discharges calculated by Models I and II (u_*/w_s and v_t/w_s) for channel inclinations of (a) 15° and (b) 20°.

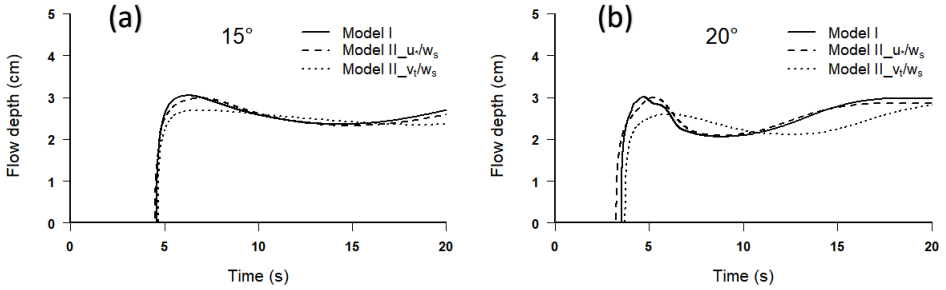

Fig. 4. Time series of flow depths calculated by Models I and II (u_*/w_s and v_t/w_s) for channel inclinations of (a) 15° and (b) 20°.

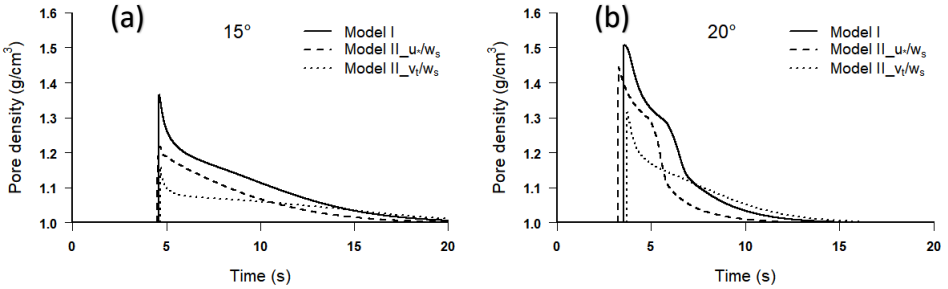

Fig. 5. Time series of pore fluid density calculated by Models I and II (u_*/w_s and v_t/w_s) for channel inclinations of (a) 15° and (b) 20°.

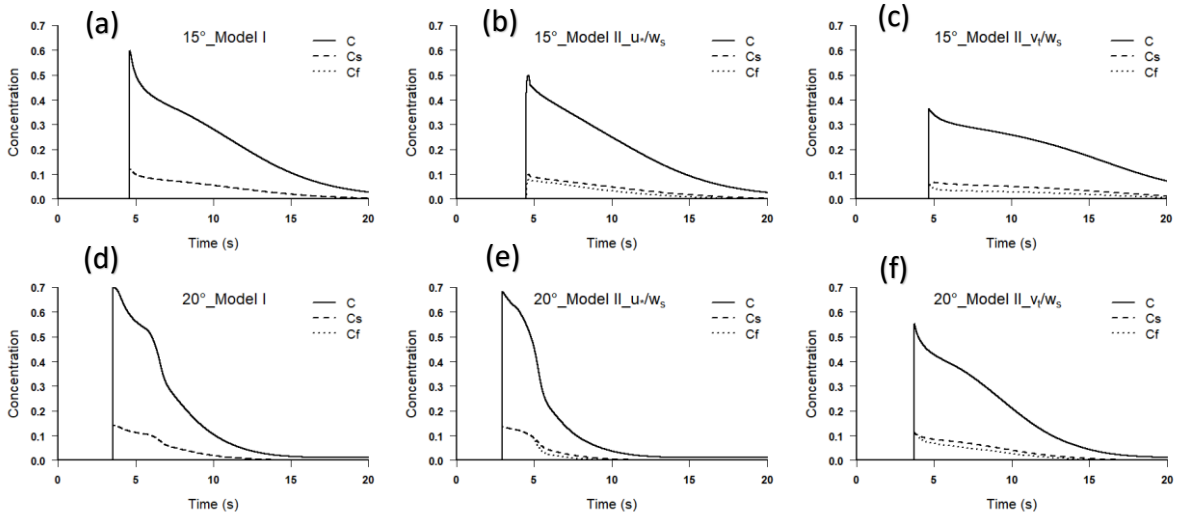

Fig. 6. Time series of concentrations of sediment mixture, small particles, and sediment particles behaving as a fluid phase calculated by Models I and II (u_*/w_s and v_t/w_s): (a) 15°, Model I; (b) 15°, Model II, v_t/w_s; (c) 15°, Model II, u_*/w_s; (d) 20°, Model I; (e) 20°, Model II_u_*/w_s; (f) 20°, Model II, v_t/w_s.

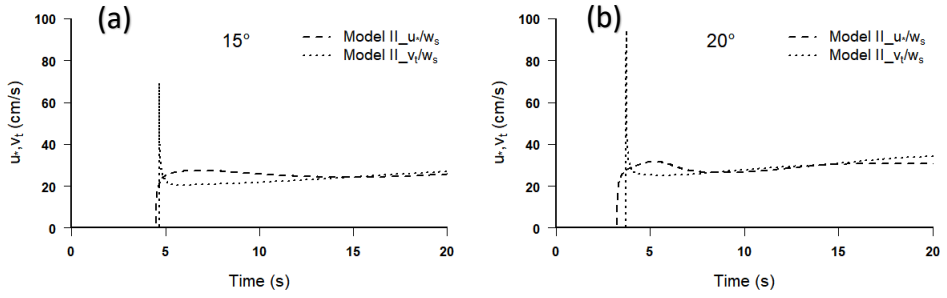

Fig. 7. Time series of u_* and v_t calculated by Model II (u_*/w_s and v_t/w_s) for channel inclinations of (a) 15° and (b) 20°.

4. Conclusion

In this work, we constructed numerical simulation model of debris flows focusing on the transitional behavior of fine sediment and compared its performance with existing models. We conducted numerical simulations of debris flows with bidisperse granular materials, employing two models for the behavior of small particle. Hydrographs of the two models were significantly different at higher slopes, with a sharp peak at the front of debris flows in Model I results and a relatively moderate peak in those of Model II. These differences are caused by higher pore fluid densities from the front to the tail of debris flows in Model I, in contrast to the lower pore fluid density observed in the Model

II results, where not all small particles behaved as a fluid phase. These results indicate that the debris flow discharge rates can be overestimated especially at higher slopes, if the transitional behavior of fine sediment is not appropriately considered.

The sensitivity analysis conducted in this study addressed relatively limited conditions, such that further investigation may be needed to decide whether u_*/w_s or v_t/w_s in Model II leads to better performance. This study focused only on the erosion process; however, the deposition process should be also investigated in future studies.

Acknowledgements

This work was partly supported by Grant-in-Aid for JSPS Fellows Grant Number 17J08424 and by a grant from the Ministry of Land, Infrastructure, Transport and Tourism, Japan.

References

Berzi, D., and Jenkins, J. T., 2008, A theoretical analysis of free-surface flows of saturated granular-liquid mixtures: Journal of Fluid Mechanics, v. 608, p. 393–410, doi:10.1017/S0022112008002401.

Berzi, D., and Larcan, E., 2013, Flow resistance of inertial debris flows: Journal of Hydraulic Engineering, v. 139, no. 2, p. 393–410, doi: 10.1061/(ASCE)HY.1943-7900.0000664.

Coe, J. A., Kinner, D. A., and Godt, J. W., 2008, Initiation conditions for debris flows generated by runoff at Chalk Cliffs, central Colorado: Geomorphology, v. 96, p. 270–297, doi:10.1016/j.geomorph.2007.03.017.

Egashira, S., Miyamoto, K., and Itoh, T., 1997, Constitutive equations of debris flow and their applicability, *in* Proceedings, 1st Int. Conf. on Debris Flow Hazards Mitigation: Mechanics, Prediction, and Assessment, C. L. Chen, ed.: ASCE, New York, p. 340–349.

Egashira, S., Honda, N., and Itoh, T., 2001, Experimental study on the entrainment of bed material into debris flow: Physics and Chemistry of the Earth (C), v. 26, no. 9, p. 645–650.

Hotta, N., 2011, Pore water pressure distributions of granular mixture flow in a rotating mill, *in* Italian Journal of Engineering Geology and Environment, R. Genevois, D. L. Hamilton, and A. Prestininzi, eds.: Sapienza Universita Editrice Univ. Press, Rome, Italy, p. 319–330.

Hotta, N., Kaneko, T., Iwata, T., and Nishimoto, H., 2013, Influence of fine sediment on the fluidity of debris flows, Journal of Mountain Science, v. 10, no. 2, p. 233–238, doi: 10.1007/s11629-013-2522-y.

Iverson, R. M., 1997, The physics of debris flows, Review of Geophysics, v. 35, no. 3, p. 245–296.

Iverson, R. M. and Ouyang, C., 2015, Entrainment of bed material by Earth-surface mass flows: Review and reformulation of depth-integrated theory: Review of Geophysics, v. 53, p. 27–58, doi:10.1002/2013RG000447.

Kaitna, R., Palucis, M. C., Yohannes, B., Hill, K. M., and Dietrich, W. E., 2016, Effects of coarse grain size distribution and fine particle content on pore fluid pressure and shear behavior in experimental debris flows: Journal of Geophysical Research: Earth Surface, v. 121, p. 415–441.

Nakatani, K., Furuya T., Hasegawa Y., Kosugi K., and Satofuka, Y., 2018, Study on fine sediment phase change factors and influence on debris flow behavior: Journal of the Japan Society of Erosion Control Engineering, v. 70, no. 6, p. 3–11. (in Japanese with English summary)

Nishiguchi, Y., Uchida, T., Tamura, K., and Satofuka, Y., 2011, Prediction of run-out process for a debris flow triggered by a deep rapid landslide, *in* Italian Journal of Engineering Geology and Environment, R. Genevois, D. L. Hamilton, and A. Prestininzi, eds.: Sapienza Universita Editrice Univ. Press, Rome, Italy, p. 477–485.

Osti, R., and Egashira, S., 2008, Method to improve the mitigative effectiveness of a series of check dams against debris flows: Hydrological Processes, v. 22, p. 4986–4996, doi: 10.1002/hyp.7118.

Osti, R., Egashira, S., and Itoh, T., 2004, Prediction of 1999-San Julian debris flows based on dependent and independent occurrences: Annual Journal of Hydraulic Engineering, JSCE, v. 48, p. 913–918.

Sakai, Y., Hotta, N., Kaneko, T., and Iwata, T., 2019, Effects of grain-size composition on flow resistance of debris flows: behavior of fine sediment : Journal of Hydraulic Engineering, v. 145, no. 5, doi: 10.1061/(ASCE)HY.1943-7900.0001586.

Takahashi, T., 1991, Debris flow, Balkema, Rotterdam, Netherlands.

Takahashi, T., Nakagawa, H., Harada, T., and Yamashiki, Y., 1992, Routing debris flows with particle segregation: Journal of Hydraulic Engineering, v. 118, no. 11, p. 1490–1507, doi:10.1061/(ASCE)0733-9429(1992)118:11(1490).

Uchida, T., Nishiguchi, Y., Nakatani, K., Satofuka, Y., Yamakoshi, T., Okamoto, A., and Mizuyama, T., 2013, New numerical simulation procedure for large-scale debris flows (Kanako-LS), International Journal of Erosion Control Engineering, v. 6, no. 2, p.58–67.